

Solid-Solid Phase Change Material Composite Based Cylindrical Heat Sink For Transient Cooling

Midhun V C¹, Sandip K Saha¹

¹ Department of Mechanical Engineering, IIT Bombay, Mumbai-420007, India
midhunvc@iitb.ac.in; sandip.saha@iitb.ac.in

Abstract - Phase change material-based heat sinks are a practical solution for transient passive cooling of electronic packages and battery thermal management systems. This work analysed heat transfer in the solid-solid phase change material (SSPCM) composite-based cylindrical heat sink using the modified enthalpy porosity method incorporated in the numerical model. This study performs a numerical analysis of two-dimensional transient heat transfer in a cylindrical heat sink filled with SSPCM. Neopentyl Glycol (NPG) is used as the SSPCM, which undergoes the solid-to-solid transition from α phase to γ phase by absorbing thermal energy and releasing heat during the phase transition in the reverse direction. The cylindrical heat sink cavity is packed with SSPCM composite comprised of NPG with 3 w/w% of copper oxide (CuO) nanoparticles as the thermal conductivity enhancer. In this work, the effect of fin parameters of the heat sink and the heat dissipation rate over the safe operational time with a safe temperature limit of 80 °C are considered for the analysed. The influence of cavity angle, fin angle, and the heat flux over the safe operational time and thermal energy storage utilisation are analysed in detail. From the numerical simulation results, the effect of heat flux and the fin parameters are evident over the safe operational period and the distribution of the phase transition fraction of the SSPCM composite. The SSPCM composite-based cylindrical heat significantly improved the safe operational time.

Keywords: Solid-solid phase change material, heat sink, thermal management, safe operational time, fin parameters

1. Introduction

Thermal management is an essential issue for current electronic packaging systems, directly impacting their performance. Researchers and industrialists have placed a high value on it. It becomes increasingly difficult to prevent thermal imbalance brought on by insufficient heat removal techniques when the power density of electronic components increases. As a result, scientists concentrate on creating thermal management systems that are smaller and more efficient. Heat sinks based on phase change materials (PCMs) have grown in popularity recently. Researchers have conducted experimental and numerical testing of PCM-based heat management techniques [1], [2].

Saha et al. [3] investigated the impact of varying percentages of thermal conductivity enhancers (TCE) in the form of pin fins on the thermal performance of a PCM-filled heat sink. Their findings indicated that an 8% TCE concentration performed better than other combinations. In another study, Baby and Balaji [4] performed a transient experimental analysis on the heating and cooling phases of n-eicosane as a PCM using a plate-finned heat sink under a constant power level of 5–10 W, which corresponds to a heat flux of 2–4 kW/m². They reported that the PCM maintained the heat sink temperature below 50 °C for up to 90 minutes of operation. Fok et al. [1] conducted a similar study using eicosane as the PCM and found that the PCM was effective at lower power levels (3–5 W) due to its low melting point between 35–40 °C. Midhun et al. [5] conducted a numerical study to optimise a plate-fin heat sink packed with solid-solid phase change material for the thermal management of electronic cooling and found that 26% of the thermal conductivity enhancer is suitable for giving the maximum operational time.

In electronics packaging, PCM-based heat sinks face challenges such as PCM leakage and complex heat sink designs, which can decrease the system's efficiency and reliability. The most promising solid-solid PCMs include polyethylene, polyalcohols, and perovskites. Within the polyalcohol group, neopentyl glycol (NPG), pentaerythritol (PE), and tri-hydroxymethyl-aminomethane (TAM) are commonly used solid-solid PCMs due to their relatively high transition enthalpies during the solid-solid phase change [6], [7], [8]. NPG, an organic compound (C₅H₁₂O₂), undergoes a solid-state phase change between 40 and 48 °C, transitioning from a tetragonal to a cubic structure. It can absorb significant heat during this solid-solid

transition, primarily through hydrogen bond interactions. Although these solid-solid phase change materials (SSPCM) show promise as heat sink materials due to their heat storage and release capabilities, their performance is limited by low thermal conductivity. To address this, researchers have found that incorporating conductive particles or thermal conductivity-enhancing additives can effectively improve the thermal conductivity of the PCM [9]. Midhun et al. [5] introduced the modified enthalpy porosity method for the numerical heat transfer study of a SSPCM composite-filled flat plate heat sink for the thermal management of electronics packages. The effect of various fin parameters over the SOT was also investigated, and a 26% thermal conductivity enhancer was reported as the optimum value for plate fins in the heat sink. However, the scope of SSPCM composites in radial fins under high heat flux conditions still needs to be explored.

This study aims to investigate the SSPCM phase transition within cylindrical heat sinks used for high-power transient cooling. A two-dimensional (2D) numerical model of the SSPCM-based cylindrical heat sink will be developed to examine the impact of different geometric and thermal parameters.

2. Materials and Method

The present work focuses on the two-dimensional geometry of various radial fin heat sink configurations. NPG with a 3% (w/w) CuO additive is used as the solid-solid phase change material (SSPCM) to enhance thermal conductivity. The properties of NPG + 3% (w/w) CuO composite and the Aluminium as the radial fin material acting as the TCE are listed in Table 1.

Table 1. Material Properties

Materials	T_i (K)	ρ (kg/m ³)	k (W/m K)	C_p (J/kg K)
Aluminium [3]	-	2712.9	179.6	960
SSPCM composite [10]	313.05-318.25	1150	0.61	2389

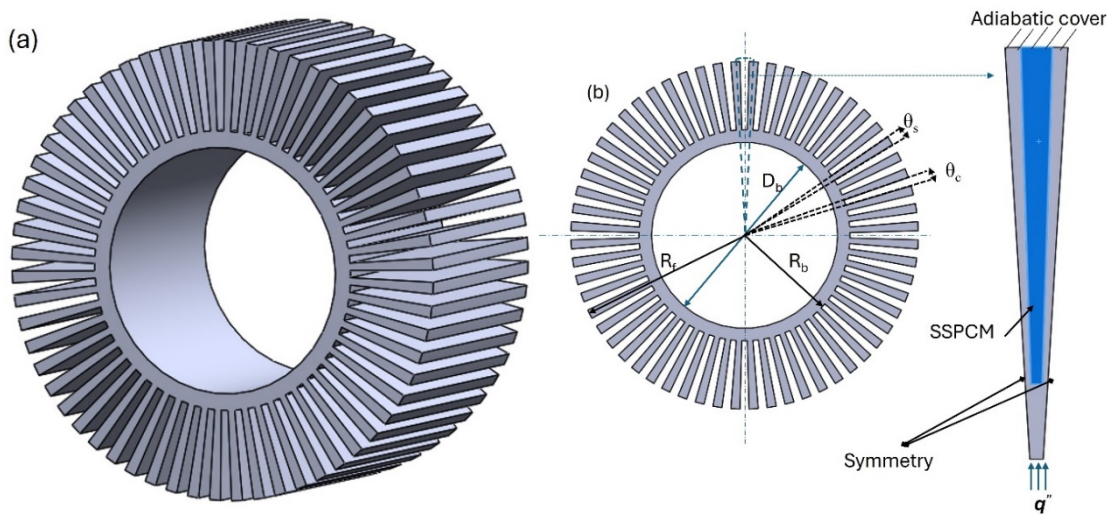


Fig. 1: Radial fin arrangement and the computational domain.

Table 2. Fin configurations

%SSPCM	%TCE	N	θ_c ($^\circ$)	θ_s ($^\circ$)
100	0	0	6	0
72	28	60	5	1
44	56	60	3	3
13	71	60	2	4

Figure 1(a) and (b) show the details of the radial fin heat sink. From [11], the base diameter of the heat sink is fixed at 30 mm and the outer radius at 26 mm. In the radial fins, the gap between the fins is packed with the SSPCM composite. The inner and outer radius of this cavity is represented as $R_b = 17$ mm, and the outer fin radius is $R_f = 26$ mm. The cavity angle (θ_c) and the heat sink fin angle (θ_s) are varied throughout the simulation study for different heat flux conditions. The base region of the heat sink is provided with the constant heat flux condition, while the outer circumference of the heat sink and the cavity is provided with the constant heat flux condition. Table 2 depicts the different percentages of TCE and SSPCM combinations in a unit cell of the radial fin heat sink with the number of fins (N) limited to 60. These combinations are investigated at 25000, 50000, and 75000 W/m² heat fluxes.

2.1. Numerical Model

In this study, only the solid-solid phase transition of the SSPCM is considered, making the entire numerical analysis as a heat transfer with transient conduction mode. The numerical model is applied based on the following assumptions: (i) heat sink thermal properties are considered constant and isotropic, (ii) heat transfer within the radial fin heat sink is treated as a two-dimensional phenomenon by disregarding end effects in the z-direction.

$$\frac{\partial (\rho h)}{\partial t} = k \nabla^2 T \quad (1)$$

where, the ρ represents the density, and h denotes the specific enthalpy. The specific enthalpy, h , comprises both the sensible and enthalpy associated with the phase transition.

$$h = h_{ref} + \int_{T_{ref}}^T C_p dT + \beta \Delta h \quad (2)$$

where, h_{ref} , C_p and T_{ref} represent the reference specific enthalpy, specific heat, and reference temperature, respectively. β denotes the fraction of phase transition from α solid phase to the γ solid phase, and this can be determined by using the following equation.

$$\beta = \begin{cases} 0 & \text{if } T < T_\alpha \\ \frac{T - T_\alpha}{T_\gamma - T_\alpha} & \text{if } T_\alpha < T < T_\gamma \\ 1 & \text{if } T > T_\gamma \end{cases} \quad (3)$$

A second-order upwind scheme is employed for the spatial discretisation of the energy equation. The convergence criterion for the energy equation is set to 10^{-6} . The equations mentioned above are solved using Ansys Fluent 2022 R1.

2.2. Boundary conditions and grid independence study

The initial temperature across the entire computational domain is established at 296.5 K. Adiabatic conditions are applied on the circumference wall of the heat sink filled with the SSPCM composite inside the cavity. Additionally, the bottom surfaces of the heat sink are subjected to different high levels of heat flux ranging from 25000 W/m² to 75000 W/m². The entire simulation is conducted after the grid independence study for the SSPCM composite packed radial heat sink for different grid sizes ranging from coarse mesh to fine mesh. The grid size ranging from 0.3 mm to 0.05 are conducted. A 0.1 mm grid size provided the maximum temperature difference below 0.01 K. The time step size is taken as 1s after conducting the time step independence study for the selected grid size from the grid independence study.

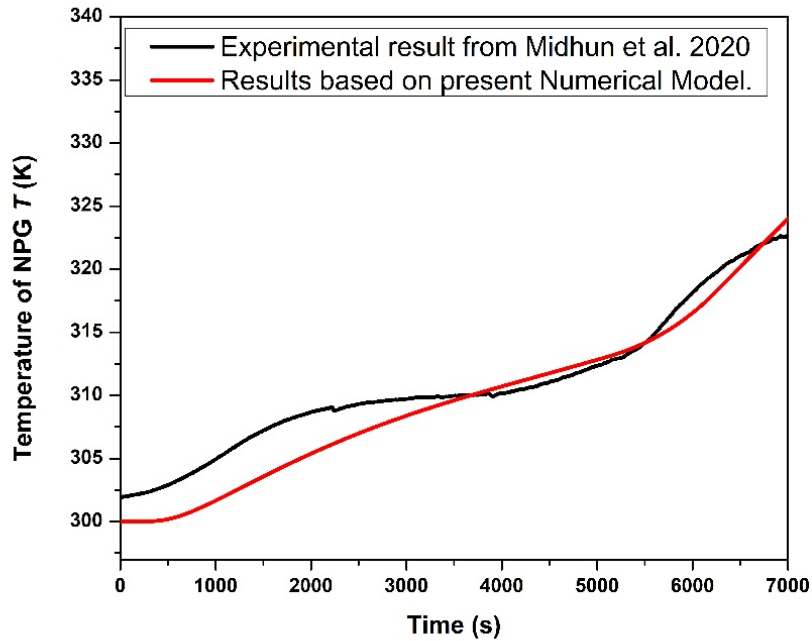


Fig. 2: Validation of the numerical model.

3. Results and Discussions

3.1. Thermal Response and Spatial Temperature Distribution

Figure 3 illustrates the temperature profile of an 8% TCE with a 3-fin SSPCM-based heat sink configuration operating at 4 W. The graph plots the thermal response of the SSPCM-based heat sink at various locations. The highest temperature is recorded at the bottom circumference (Location 1) throughout the operation. Also, the temperature profile from Location 2 coincides with Location 1 due to the high thermal conductivity of the aluminium fin acting as the TCE. A gradual temperature decrease along the radial direction indicates significant heat transfer upwards through the heat sink. The lowest temperature is observed at Location 4, where the top surface is assumed to be insulated. The temperature-time plot at Locations 1-4 shows the SSPCM undergoing a solid-solid phase transition. During this phase, the SSPCM absorbs thermal energy, which helps slow the temperature rise of electronic packages or heat-dissipating devices. This effect is evident from the change in the slope of the temperature-time curve at Point 1. After a certain period, the slope increases and reaches the setpoint temperature, indicating the maximum steady-state operating temperature (SOT). Thus, the heat sink effectively utilises the SSPCM's thermal energy storage capacity to extend its operational period. The case of 100% SSPCM (without radial fins – W/O_RF) is also included as a reference for comparison and is also shown in the $T-t$ plot, indicating its very low safe operational time. Here, the SOT improvement through the radial fins is evident in high-power density cases.

The mechanism of heat transfer enhancement through the use of radial fins in SSPCM-based radial heat sinks with 71% TCE can be analysed from Fig. 4. During the initial stages of the transient analysis, the SSPCM in the heat sink stores sensible heat until it reaches the onset of phase transition. A two-dimensional temperature gradient can be observed from the temperature contour plot. The heat transfer from the radial fin acting as the thermal conductivity enhancer is clearly visible. Also, the temperature difference is less or better due to the TCE, and temperature uniformity between the SSPCM composite and the fins can be observed.

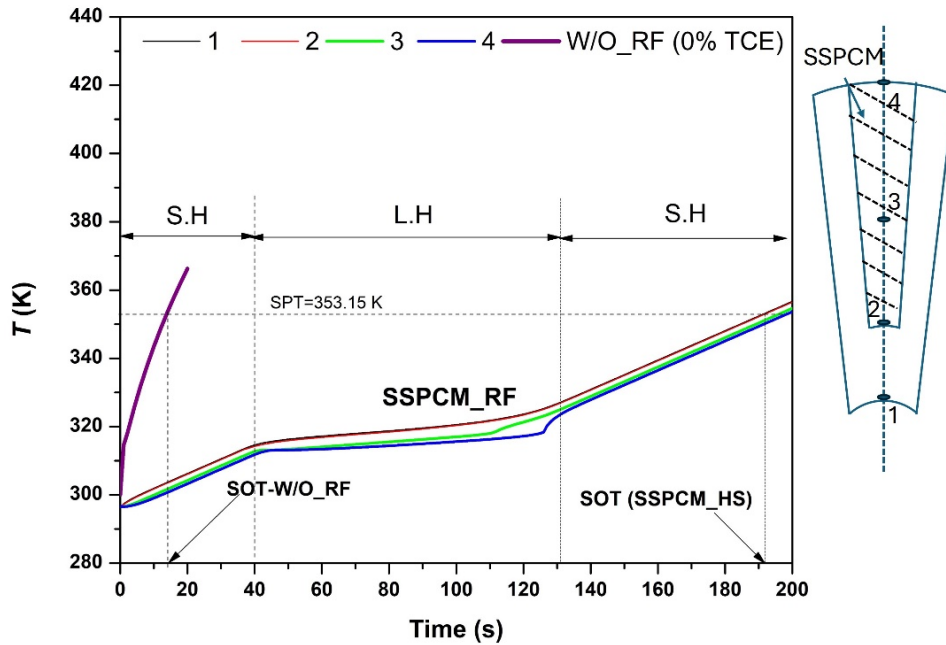


Fig.3: T-t plot for various locations (1 to 4).

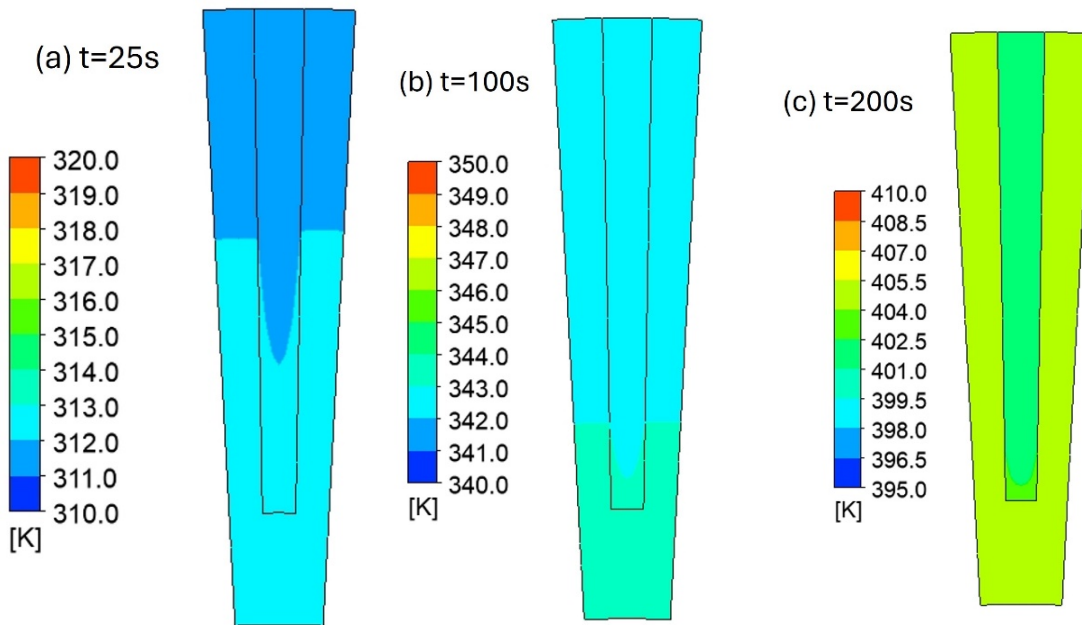


Fig. 4. Temperature distribution at (a) $t=25$ s, (b) $t=100$ s, and (c) $t=200$ s for 71 % TCE.

The heat transfer through the fins from the base circumference acting as the source has effectively utilised the thermal storage capacity of the SSPCM. The β phase fraction of the SSPCM within the radial heat sink increases over time, which is evident from Fig. 5. Heat conducted from the base of the HS and distributed by the fins is stored as thermal energy during the SSPCM's solid-solid (α - γ) phase transition. The phase transition contours clearly indicate that both heat conduction through the fins and the SSPCM are crucial in maximising the SSPCM's thermal energy storage capacity. Unlike solid-liquid

PCM, the temperature and phase transition contours show that heat conduction through the SSPCM is significant. The temperature contour also reveals lateral symmetry about the middle axis, indicating two-dimensional heat flow within the heat sink.

All four configurations are illustrated in Fig. 6. The SOT analysis provides a detailed examination of the thermal response of different heat sinks over time as they reach the safe operational temperature limit of 80 °C under varying heat flux. The analysis reveals a significant decrease in SOT with increasing power levels. At 25,000 and 50,000 W/m², the percentage change of TCE is significantly evident. Radial fins improve the SOT ninefold compared to the 0% TCE case. However, under these heat flux conditions, the increase in TCE reduces the SOT after a specific limit due to the reduction in thermal energy storage capacity by the percentage of SSPCM reduction. At 75000 W/m², the percentage change of %TCE has minimal effect on SOT improvement. However, the reduction in SOT with an increase in TCE is minimal. Instead, a consistently low SOT can be observed, indicating the necessity of a high thermal diffusive medium at high heat flux conditions. In this analysis, a fixed number of fins is considered; therefore, to better understand the effect of TCE over SOT, further study must be conducted by varying the number of fins.

3.2. Safe operational time variation

All four configurations are illustrated in Fig. 6. The SOT analysis provides a detailed examination of the thermal response of different heat sinks over time as they reach the safe operational temperature limit of 80 °C under varying heat flux. The analysis reveals a significant decrease in SOT with increasing power levels. At 25,000 and 50,000 W/m², the percentage change of TCE is significantly evident. Radial fins improve the SOT ninefold compared to the 0% TCE case. However, under these heat flux conditions, the increase in TCE reduces the SOT after a specific limit due to the reduction in thermal energy storage capacity by the percentage of SSPCM reduction. At 75000 W/m², the percentage change of %TCE has minimal effect on SOT improvement. However, the reduction in SOT with an increase in TCE is minimal. Instead, a consistently low SOT can be observed, indicating the necessity of a high thermal diffusive medium at high heat flux conditions. In this analysis, a fixed number of fins is considered; therefore, to better understand the effect of TCE over SOT, further study must be conducted by varying the number of fins.

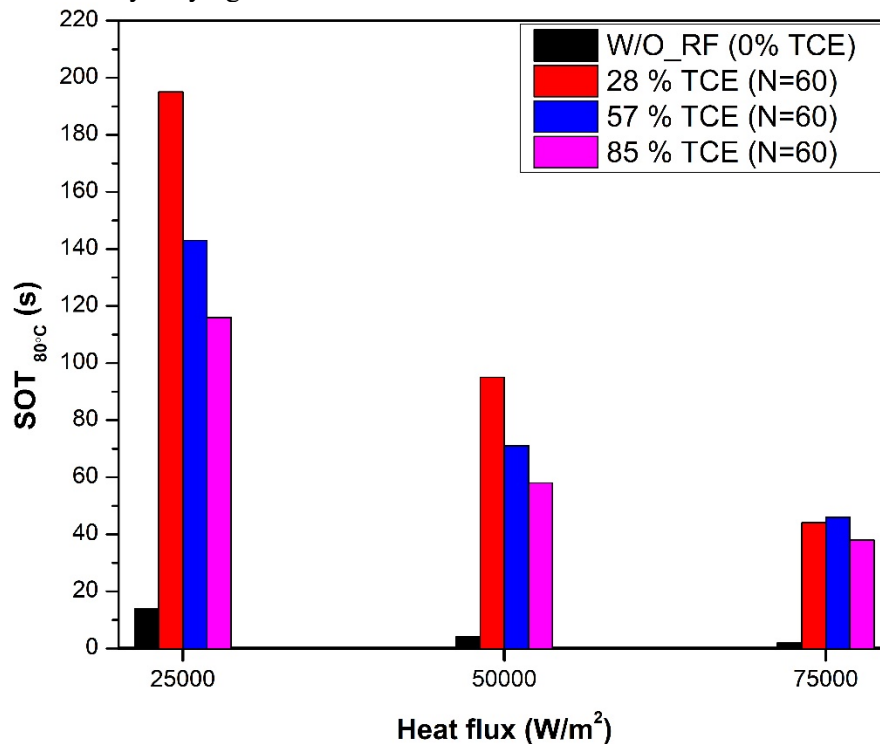


Fig. 6: SOT variation with different heat flux and %TCE.

4. Conclusion

A two-dimensional transient heat transfer is accomplished for a radial heat sink packed with SSPCM composite for thermal management at high power density situations. The effect of the radial fins acting as TCE is observed. Also, the variation of the cavity angle and the fin angle for a fixed number of fins under different heat flux conditions are analysed. Under higher heat dissipation cases, SSPCM with radial fin configurations improves the SOT to a maximum of sixteen to twenty-two times, with the heat flux ranging from 25000 to 50000 W/m² compared to the reference case of 0% TCE. Overall, the %TCE effect is significant, especially at high heat flux conditions, and further study can be conducted by varying the number of fins and the base thickness under high heat flux conditions.

NOMENCLATURE

c_p	specific heat	J/(kg · K)
h	heat transfer coefficient	W/(m ² · K)
h_{ref}	Reference specific enthalpy	J/(kg.K)
k	Thermal conductivity	W/(m.K)
N	Number of fins	
T	Temperature	K
t	time	s
β	Phase fraction	
Δh	Phase transition enthalpy	kJ/kg
θ	fin angle	°
ρ	Density	kg/m ³

Subscripts

c	cavity
ref	reference
s	radial fin
t	phase transition

Acknowledgements

We thank the financial support (EEQ/2021/000004) from the Department of Science and Technology, Government of India.

References

- [1] S. C. Fok, W. Shen, and F. L. Tan, "Cooling of portable hand-held electronic devices using phase change materials in finned heat sinks," *Int. J. Therm. Sci.*, vol. 49, no. 1, pp. 109–117, 2010, doi: 10.1016/j.ijthermalsci.2009.06.011.
- [2] R. Kandasamy, X. Q. Wang, and A. S. Mujumdar, "Transient cooling of electronics using phase change material (PCM)-based heat sinks," *Appl. Therm. Eng.*, vol. 28, no. 8–9, pp. 1047–1057, 2008, doi: 10.1016/j.applthermaleng.2007.06.010.
- [3] S. K. Saha, K. Srinivasan, and P. Dutta, "Studies on optimum distribution of fins in heat sinks filled with phase change materials," *J. Heat Transfer*, vol. 130, no. 3, pp. 1–4, 2008, doi: 10.1115/1.2804948.
- [4] R. Baby and C. Balaji, "Thermal performance of a PCM heat sink under different heat loads: An experimental study," *Int. J. Therm. Sci.*, vol. 79, pp. 240–249, 2014, doi: 10.1016/j.ijthermalsci.2013.12.018.
- [5] V. C. Midhun, M. Maroliya, and S. K. Saha, "Numerical investigation and optimisation of solid–solid phase change material composite-based plate–fin heat sink for thermal management of electronic package," *Appl. Therm. Eng.*, vol. 248, no. PA, p. 123183, Jul. 2024, doi: 10.1016/j.applthermaleng.2024.123183.
- [6] K. P. Venkitaraj, B. Praveen, H. Singh, and S. Suresh, "Low melt alloy blended polyalcohol as solid-solid phase

- change material for energy storage: An experimental study,” *Appl. Therm. Eng.*, vol. 175, no. April 2019, p. 115362, 2020, doi: 10.1016/j.applthermaleng.2020.115362.
- [7] J. D. Webb and R. W. Burrows, “Materials Research for Passive Solar Systems: Solid-State Phase-Change Materials,” 1985.
- [8] K. P. Venkataraj and S. Suresh, “Experimental thermal degradation analysis of pentaerythritol with alumina nano additives for thermal energy storage application,” *J. Energy Storage*, vol. 22, no. January, pp. 8–16, 2019, doi: 10.1016/j.est.2019.01.017.
- [9] K. P. Venkataraj, S. Suresh, B. Praveen, and S. C. Nair, “Experimental heat transfer analysis of macro packed neopentylglycol with CuO nano additives for building cooling applications,” *J. Energy Storage*, vol. 17, pp. 1–10, 2018, doi: 10.1016/j.est.2018.02.005.
- [10] B. Praveen and S. Suresh, “Experimental study on heat transfer performance of neopentyl glycol/CuO composite solid-solid PCM in TES based heat sink,” *Eng. Sci. Technol. an Int. J.*, vol. 21, no. 5, pp. 1086–1094, 2018, doi: 10.1016/j.jestch.2018.07.010.
- [11] J. H. Jeong, S. Hah, D. Kim, J. H. Lee, and S. M. Kim, “Thermal analysis of cylindrical heat sinks filled with phase change material for high-power transient cooling,” *Int. J. Heat Mass Transf.*, vol. 154, p. 119725, 2020, doi: 10.1016/j.ijheatmasstransfer.2020.119725.
- [12] V. C. Midhun, S. Suresh, B. Praveen, and R. S. Shiju, “Experimental study on phase transition behaviour of shape stable phase change material for application in vacuum insulation panel,” *J. Energy Storage*, vol. 32, no. July, p. 101825, Dec. 2020, doi: 10.1016/j.est.2020.101825.